ELSEVIER

Nuclear Instruments and Methods in Physics Research A 409 (1998) 167–172

NUCLEAR INSTRUMENTS & METHODS IN PHYSICS RESEARCH Section A

Design and operation of a fast high-granularity silicon detector system in a high-radiation environment

B. Alessandro[a], M. Alexeline[b], C. Baglin[b], S. Beolé[a], E. Bollito[a], G. Bonazzola[a], A. Bussière[b], V. Capony[b], W. Dąbrowski[c], P. De Remigis[a], J. De Witt[d], M. Forlen[b], P. Giubellino[a], M. Idzik[a,*], A. Marzari-Chiesa[a], M. Masera[a], W. Prado da Silva[a], L. Ramello[a], P. Rato Mendes[a], L. Riccati[a], M.S. Sartori[a], M. Sitta[a]

[a] *INFN, Torino, Italy*
[b] *LAPP, Annecy, France*
[c] *Faculty of Physics and Nuclear Techniques, Academy of Mining and Metallurgy, Cracow, Poland*
[d] *SCIPP, Santa Cruz, USA*

Abstract

We have designed, realized and operated a fast silicon detector system (50 MHz sampling frequency) to measure the angular distribution and the multiplicity of charged secondaries produced in high-energy Pb–Pb interactions, within the NA50 experiment. We present here the detector design, discuss some of the problems faced during the commissioning and report on the first results on the operation of the full system. In particular, the questions related to the operation of an integrated high-speed binary readout in a high-radiation environment (10^{14} particles/cm^2 and about 10 Mrads) and to the radiation effects on the system during the run will be addressed.

1. Introduction

NA50 [1] is a fixed target experiment investigating the production of resonances decaying to dimuons produced in high-energy (158 A GeV/c) Pb–Pb interactions at the CERN SPS. The aim is to study nuclear matter under extreme energy density conditions, having as an ultimate goal the detection of signals coming from a possible phase transition between a quark–gluon plasma and hadronic matter. In particular, the experiment is looking for dimuon production from charmonium resonances and its suppression due to Debye screening in the deconfined quark–gluon matter. The main component of the experiment is a high resolution muon spectrometer based on a toroidal magnet. Other detector subsystems are: a zero-degree calorimeter for forward energy measurements, an electromagnetic calorimeter for transverse energy measurements and a silicon microstrip detector system (MD) for charge multiplicity measurements and recognition of the target where the interaction took place. The target is segmented into seven subtargets to limit the reinteractions of the

* Corresponding author.

0168-9002/98/$19.00
PII S0168-9002(98)00079-5

secondaries. For target identification there is also a dedicated system of quartz Cherenkov counters. Other detectors are used for the incoming beam definition and pileup rejection. In order to collect sufficient statistics of J/ψ and ψ' mesons during the 1996 Pb run the experiment has been operating with the maximum available intensity 10^7 beam particles/s and with a target of 32% of an interaction length.

2. Detector specifications and assembly

The layout of the NA50 experiment has put several important constraints on the design of the silicon multiplicity detector. They can be divided into four groups:

1. *Speed*. Given the low cross-section for J/ψ production, the experiment must function at very high rate, and therefore, the deadtime of the readout electronics must be very short (50 ns). As a solution very fast binary readout electronics was chosen. It consists of an analog and a digital chip. The former (FABRIC) [2] includes preamplifier ($T_{peak} = 15$ ns), shaper and discriminator, while the latter (CDP) [3] is a digital buffer working with sampling frequency 50 MHz.

2. *Space*. The need to suppress the background due to the decays of π and K mesons imposes positioning an absorber very close to the target, and therefore a very small space available for the silicon detectors. We have designed two discs (MD1, MD2) of radial silicon microstrip detectors, 10 cm from each other. The inner radius of the detectors in each disc is 0.5cm while the outer radius is 8.5 cm.

3. *Number of particles*. The detector granularity is mainly determined by occupancy, which we decided to keep below 30%, in order to achieve a good resolution. Taking into account also multiple scattering in the target and size of the beam ($\sim$0.3 mm) we have chosen constant segmentation of the detector $\Delta\eta = 0.02$ in pseudorapidity and $\Delta\phi = 10^\circ$ in azimuthal angle.

4. *Radiation*. Estimated fluences and doses for the innermost part of the detector are, respectively, 10^{14} particles/cm^2 and 10 Mrads, while for the front-end electronics region respectively 10^{12} particles/cm^2 and 200 krads. We have decided to design full-custom rad-hard front-end electronics which includes the FABRIC produced in bipolar Tektronix technology and the CDP produced in rad-hard 0.8 μm Honeywell CMOS.

In Fig. 1 one side of one disc of the detector is shown. It is seen that there are two crowns, inner and outer. The inner crown is built of inner boards (Board 1), each including 256 channel AC-coupled detector and four couples of 64-channel analog and digital chips. Each outer board (Board 2) consists of a 128 channel DC-coupled detector and two couples of front-end electronics chips (behind the inner boards, not seen on the picture). The complete system has 13 824 channels, which include 9216 channels of 36 inner detectors and 4608 channels of 36 outer detectors, read out by 216 64-channel couples of FABRIC-CDP.

All the components of the MD were designed in the years 1992–1994 [4], [5], and data were taken with Pb ions in 1994 with a small setup, and in 1995 (at 25 MHz) with about half of the full system, which was finally operational in 1996. Assembly and testing of the detector proceeded along the following steps:

- test of individual components: detectors, boards, FABRIC (using probe cards), CDP (using probe cards – the input stage was not tested and for this reason $\sim$20% of the CDPs had to be replaced later);
- assembly and bonding in Torino: we had to perform a lot of debugging, largely due to the kapton cable connections, which appeared to be not reliable for our system;
- test of assembled boards with laser, with replacement of malfunctioning chips.

While single boards operated easily at 50 MHz, bringing the full system from 25 to 50 MHz required a complete redesign of the clock distribution system, improved terminations and the addition of adjustable delays. The most serious limitation of the system appeared to be the use of a single gain and threshold setting for one full detector disc ($\sim$7000 channels). For the 1998 run we plan to implement a more distributed one.

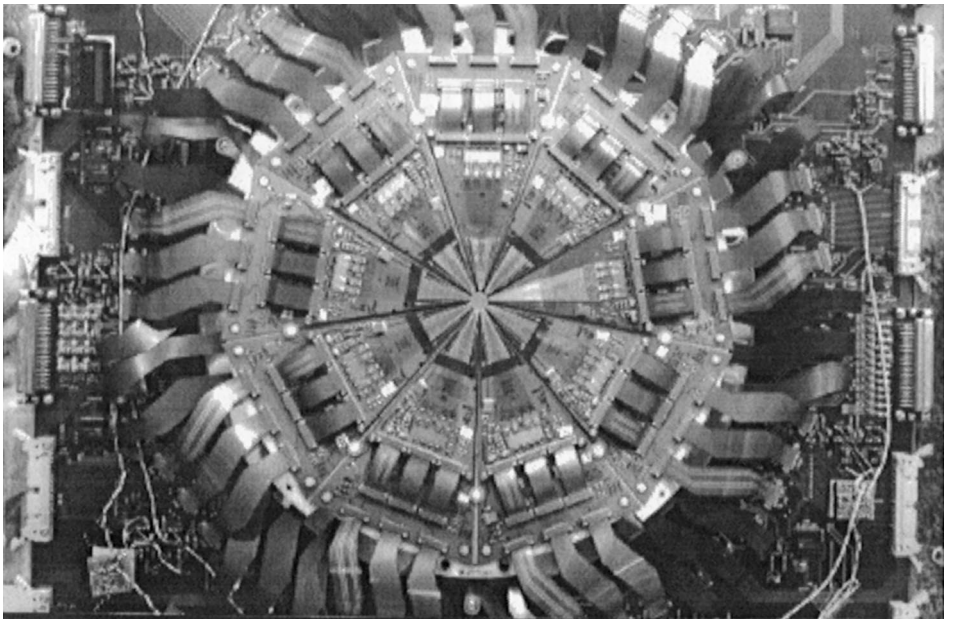

Fig. 1. Picture of the disc of the Multiplicity Detector.

3. Detector performance

In order to evaluate and optimize the detector efficiency we performed trigger delay scans and threshold scans. First a rough trigger delay scan was done changing the trigger delay in clock units and searching for maximum detector occupancy. After that the trigger delay was fixed to the one with maximum occupancy and tuned manually around the peak with few ns steps. In addition we continuously monitored the delay between multiplicity detector trigger, which was adjusted to have a fixed phase relation with our digital clock, and the experiment trigger, in order to understand better the readout performance and to set corrections for the few CDP not centered on the peak (we could set the trigger delay only for groups of 36 CDPs). In Fig. 2 the multiplicity versus monitored trigger delay for a FABRIC–CDP pair is shown. Typically there is a 20–30 ns plateau at maximum multiplicity. In order to set the correct threshold and to measure the signal-to-noise ratio (S/N) for our system, few threshold scans with and without beam were performed. Here we show the results of the last one made with a proton beam after the 1996 lead ion run. First, a noise threshold scan was done. In Fig. 3 the noise occupancy versus squared threshold for a typical chip is shown. Taking into account the statistical properties of the noise [6],

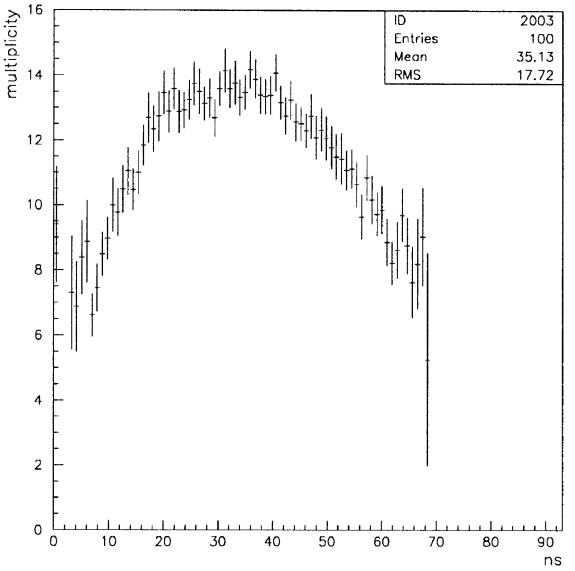

Fig. 2. Multiplicity versus delay between the experiment trigger and MD trigger for a CDP.

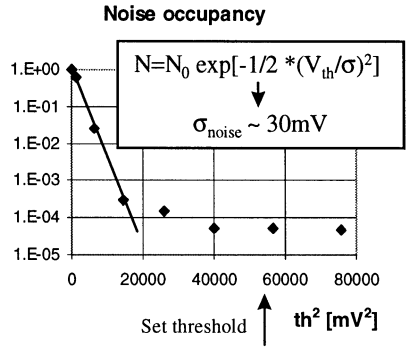

Fig. 3. Noise occupancy versus squared threshold for a FABRIC.

from the first points we estimate the gaussian noise to $\sigma_{noise} \sim 30$ mV. Above some threshold it is seen that noise saturates at a normalized occupancy below 10^{-4}. It is not clear if this saturation comes from a non-gaussian component of the noise or rather from the fact that beam was still on, although out of the region under test. Threshold scan with the proton beam on detector was then performed. In Fig. 4 the unnormalized occupancy curve and its derivative are shown. From these curves we estimate the MIP peak to be ~ 450 mV, and then the S/N ratio to be ~ 15 for our system. The threshold set was chosen a bit high (230 mV) in order to take into account some dispersion of the analog chip behavior (216 chips). In Fig. 5 preliminary results showing correlations between basic observables are shown. We can see pretty good correlation between the multiplicity per sector measured in the two multiplicity discs. Differences

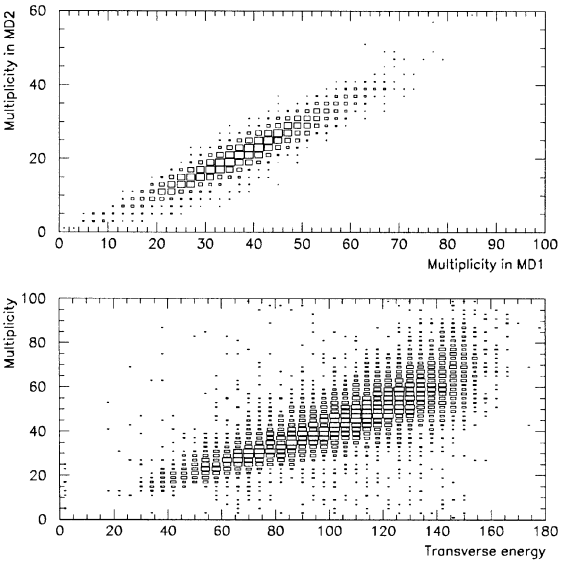

Fig. 5. Multiplicity correlations, MD1 versus MD2 and MD1 versus transverse energy.

in absolute values come mainly from the absence of efficiency corrections, the different acceptances of the discs and the decreased number of delta electrons after the first disc. Also in Fig. 5 the correlation between multiplicity in the first disc and transverse energy is presented, showing the expected good correlation.

4. Radiation effects

In the following we will report on radiation doses and fluences in the 1996 lead ion run. We should

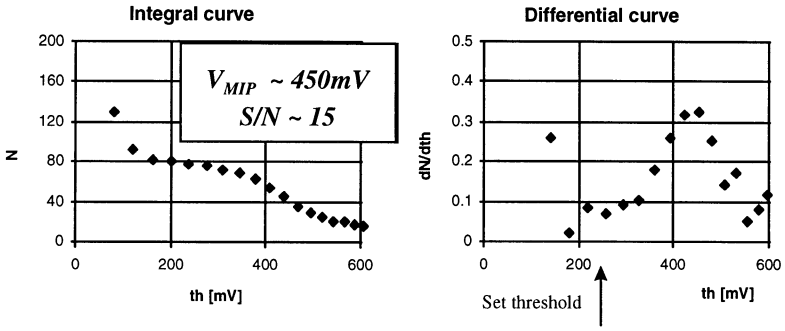

Fig. 4. Occupancy versus threshold with proton beam, after the 1996 ion run.

mention here that $\frac{5}{6}$ of the inner detectors (Board 1) were also used in the 1995 lead run, when they received roughly $\frac{1}{4}$ of the 1996 run radiation (+one year of annealing in room temperature). To estimate the radiation damage of the detectors and to apply the necessary corrections to data, at the end of the 1996 ion run we performed detector bias voltage scans. Changing detector bias we were measuring the occupancy on each strip. In Fig. 6 are shown typical curves of occupancy versus bias voltage for different strips. The first plot shows the curves for the inner detectors which were used only in the 1996 run while the second one shows the ones used in the 1995 and 1996 run. We see that, for the former, the outermost strips have depletion voltage below 20 V while the innermost strips saturate around 140 V. For the latter we can see that the innermost strips have not yet reached saturation at 160 V. Considering our nominal bias of 120 V one can see that we need to apply large efficiency corrections to the innermost strips for detectors used in the 1995 and 1996. We would like to stress that the standard p-on-n detectors we use, don't show a noticeable drop of efficiency even after high inversion, if fully depleted. Of course we do see a substantial drop of efficiency for strips which are not fully depleted. On the basis of the data from the scan we calculated the depletion voltage for each strip, as it is normally done for C–V measurements. We would like to point out here that the bias voltage scan appears to be a very powerful method, allowing to get in one shot information about the depletion voltage for each strip separately. In the upper plots of Fig. 7 typical curves of depletion voltage versus strip number (counting from the innermost) for inner and outer detectors irradiated in 1996 are shown. For the inner detector the comparison between depletion voltages obtained from bias voltage scan (at the end of run) and C–V measurements (few weeks after run) is presented, while for the outer detectors only C–V measurement results are shown. It is seen that the innermost strips of the outer detector are just before the inversion point while the outermost strips of inner detector are just after or around it. The depletion voltage values obtained from voltage scan for the outermost strips might be a bit overestimated, because for low detector bias voltage and fast front-end electronics ($T_{\text{peak}} = 15$ ns), we are dependent on the effect of ballistic deficit. From depletion voltage curves we estimate radiation fluences (including acceptor creation and donor removal, without annealing effects) which range from 10^{12} to 10^{14} eq. n/cm^2.

Coming to radiation effects on front-end electronics (for which the estimated dose was $\sim$200 krad), in the case of the analog chip we have not observed a noticeable change of performance.

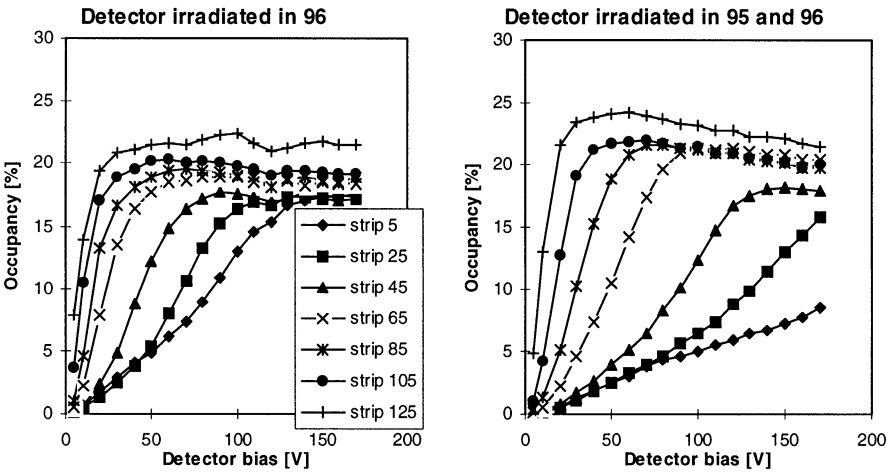

Fig. 6. Occupancy versus detector bias voltage at the end of 1996 lead ion run.

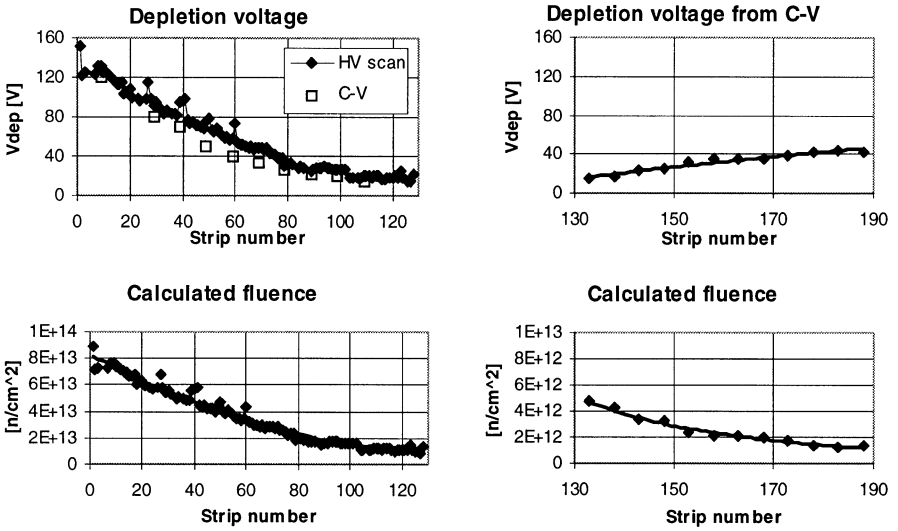

Fig. 7. Depletion voltages and calculated fluences.

We did observe changes for the outer detectors due to their DC-coupling which sent the large DC-currents (~1 μA/strip) flowing into the amplifier, changing its operation mode, and in particular the gain. Since we had the same threshold and gain control for inner and outer boards we could not correct much the operating point of one of them without affecting another. We will separate these controls for the next runs. Concerning the rad-hard digital chip we have not observed a significant degradation of performance along the run. In fact among the 216 CDP we had five non-rad-hard HP chips from the prototype production on the beam and for all of them we observed radiation-induced latchup with increasing frequency along the run. At the end of the run, three of them were not responding at all.

5. Conclusions

We have designed and operated a fast high granularity detector system in a high-radiation environment. The binary readout system has proven to be robust enough to cope with the hostile environment and allow operation with good S/N ratio. The main difficulty in our set-up originated from the radiation effects on the detectors (p-on-n), which received four times the expected fluence. At the end of the 1996 run not only all of the inner detectors were inverted but also a fraction of their innermost strips were biased below full depletion, showing a substantial drop in efficiency.

Acknowledgements

The excellent work of S. Brasolin, G. Alfarone, and M. Mucchi in the design and construction of the detector mechanics and of F. Rotondo and E. Filoni in the setting up of the electronics chain are gratefully aknowledged.

References

[1] Study of muon pairs and vector mesons produced in high energy Pb–Pb interactions, Proposal CERN/SPSLC 91-05, SPSLC/P 265, October 1991.
[2] W. Dabrowski et al., Nucl. Instr. and Meth. A 350 (1994) 548.
[3] J. DeWitt, IEEE Nuclear Science Symp. San Francisco, Oct–Nov 1993.
[4] B. Alessandro et al., Nucl. Instr. and Meth. A 360 (1995) 189.
[5] B. Alessandro et al., Nucl. Phys. B (Proc. Suppl.) 44 (1995) 303.
[6] S.O. Rice, Bell Systems Tech. J. 23 (1944) 282.